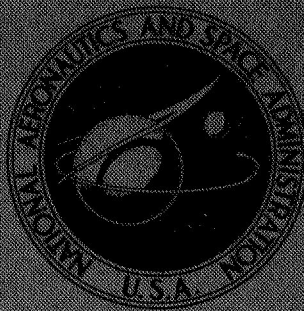


NASA TECHNICAL  
MEMORANDUM



NASA TM X-3481

NASA TM X-3481

COLD-AIR PERFORMANCE OF A TIP TURBINE  
DESIGNED TO DRIVE A LIFT FAN

II - Partial Admission

*Jeffrey E. Haas, Milton G. Kofskey,  
Glen M. Hotz, and Samuel M. Futral, Jr.*

*Lewis Research Center  
and U.S. Army Air Mobility R&D Laboratory  
Cleveland, Ohio 44135*

NATIONAL AERONAUTICS AND SPACE ADMINISTRATION • WASHINGTON, D. C. • FEBRUARY 1977

1. Report No. NASA TM X -3481	2. Government Accession No.	3. Recipient's Catalog No.	
4. Title and Subtitle <b>COLD-AIR PERFORMANCE OF A TIP TURBINE DESIGNED TO DRIVE A LIFT FAN</b> <b>II - PARTIAL ADMISSION</b>		5. Report Date February 1977	
7. Author(s) Jeffrey E. Haas, Milton G. Kofskey, Glen M. Hotz, and Samuel M. Futral, Jr.		6. Performing Organization Code	
9. Performing Organization Name and Address NASA Lewis Research Center and U.S. Army Air Mobility R&D Laboratory Cleveland, Ohio 44135		8. Performing Organization Report No. E-8914	
12. Sponsoring Agency Name and Address National Aeronautics and Space Administration Washington, D.C. 20546		10. Work Unit No. 505-05	
15. Supplementary Notes		11. Contract or Grant No.	
		13. Type of Report and Period Covered Technical Memorandum	
		14. Sponsoring Agency Code	
16. Abstract Partial admission performance was obtained for a 0.4 linear scale version of the LF460 lift fan turbine over a range of speed from 40 to 140 percent of design equivalent speed and a range of scroll inlet total to diffuser exit static pressure ratio from 2.2 to 5.0. The investigation was conducted in two parts, with each part using a different side of the turbine scroll to simulate loss of a gas generator. Each side had an arc of admission of 180°. Results are presented in terms of specific work, torque, mass flow, and efficiency.			
17. Key Words (Suggested by Author(s)) Tip turbine; Lift fan turbine; Partial admission performance; Aerodynamic performance; Efficiency; VTOL aircraft; STOL aircraft		18. Distribution Statement Unclassified - unlimited STAR Category 02	
19. Security Classif. (of this report) Unclassified	20. Security Classif. (of this page) Unclassified	21. No. of Pages 26	22. Price* A03

\* For sale by the National Technical Information Service, Springfield, Virginia 22161

# COLD-AIR PERFORMANCE OF A TIP TURBINE DESIGNED TO DRIVE A LIFT FAN

## II - PARTIAL ADMISSION

by Jeffrey E. Haas, Milton G. Kofskey, Glen M. Hotz,  
and Samuel M. Futral, Jr.

Lewis Research Center and  
U.S. Army Air Mobility R&D Laboratory

### SUMMARY

Partial admission performance was obtained for a 0.4 linear scale version of the LF460 lift fan turbine over a range of speed and pressure ratio. These cold-air tests covered a range of speed from 40 to 140 percent of design equivalent speed and a range of scroll inlet total to diffuser exit static pressure ratio from 2.2 to 5.0.

The investigation was conducted in two parts, with each part using a different side of the turbine scroll to simulate the loss of a gas generator. Each side had an arc of admission of  $180^{\circ}$ . In the first part the forward side of the scroll in which the airflow was in the same direction as the direction of rotation was used. In the second part the reverse side of the scroll in which the airflow was in a direction opposite to that of rotation was used.

The results of the investigation indicated an efficiency of 0.750 for the forward side of the turbine at design equivalent speed and pressure ratio. This efficiency was based on stator inlet total pressure and rotor exit total pressure. For the reverse side of the turbine the efficiency was 0.730. The difference in the two efficiencies was attributed to higher stator losses on the reverse side.

The average partial admission efficiency was 0.740. This was obtained by averaging the efficiencies for the forward and reverse sides. This average efficiency was 9 percent less than the full admission efficiency of 0.815. The difference was attributed to the pumping and sector losses associated with partial admission operation.

### INTRODUCTION

In the past several years a need has been demonstrated for an airplane that has the VTOL capability of a helicopter together with the advantages of the current conventional

aircraft with respect to speed, cargo capacity, and fuel economy. Use of these V/STOL aircraft for civil aviation would reduce congestion and noise pollution that exists at many large airports. For military service, V/STOL aircraft could be used for assault transport, anti-submarine warfare, search and rescue missions, and early warning systems.

Several engine and component arrangements have been considered for providing takeoff and landing lift for this type of aircraft. These are discussed in some detail in references 1 to 3. One arrangement is a fan driven by a turbine which is mounted on the rotating shroud of the fan blades. Such a turbine is called a tip-turbine and is supplied by one or more remotely located gas generators.

Some of the design features of a tip-turbine are not normally desirable for a conventional turbine design. Mounting the rotor blades on the fan shroud results in blades with hub-to-tip radius ratios in the vicinity of 0.95. Also, large rotor tip and axial clearances must be used to allow for thermal growth and considerable fan flexure. These rotor tip clearances can be as large as 25 percent of the rotor blade height. There is also some concern about losses in the scroll. The scroll is necessarily complex with each half of the scroll serving half of the stator assembly because two gas generators are used for redundancy in case one fails during takeoff or landing. The scroll is further complicated because of a requirement for the two scroll inlets to be adjacent to each other.

In order to compare the advantages and disadvantages of the lift fan system with other drive concepts, detailed performance data for the tip-turbine is required. However, at present, minimal performance data exists.

Reference 4 is the detailed design report of a lift fan program sponsored by the NASA Lewis Research Center. This particular lift fan system design, which has the designation LF460, uses a tip-turbine to drive the fan. Because of the need for detailed performance data for tip-turbines, a 0.4 linear scale version of the tip-turbine from the LF460 was fabricated and tested. A linear scale factor of 0.4 was chosen in order to use an existing Lewis Research Center cold-air component test facility. A solid disk was used in place of the fan for the test rotor. The rotor clearances were scaled to match the calculated hot running clearances of the full-size turbine. Three series of tests were planned. The first tests were general performance tests, the results of which are presented in reference 5. The second series of tests, which is the subject of this report, consisted of partial admission tests with one side of the scroll used at a time to simulate loss of one of the gas generators. The third series of tests will determine the effect of leakage from the fan into the turbine.

Reference 5 presents the results of the general performance tests. These tests were conducted over a range of speed from 40 to 140 percent of the equivalent design speed, and over a range of scroll inlet total to diffuser exit static pressure ratio from 2.0 to 4.2. At the design value of stator inlet total to rotor exit total pressure ratio, the efficiency was 0.815, compared to a design value of 0.832.

This report presents the performance results of the partial admission tests. These tests were conducted in two parts, with each part using a different side of the scroll to simulate loss of a gas generator. Each part had an arc of admission of  $180^{\circ}$ . In the first part the half of the scroll in which the airflow was in the same direction as the direction of rotation was used. In the second part the other half of the scroll in which the airflow was in a direction opposite to that of rotation was used. The airflow was in a direction opposite to that of rotation because of the requirement that the scroll inlets be adjacent to each other. In both parts, the tests were conducted over a range of speed from 40 to 140 percent of equivalent design speed, and over a range of scroll inlet total to diffuser exit static pressure ratio from 2.2 to 5.0.

In this report, results are presented as performance maps and curves relating equivalent values of mass flow and torque with pressure ratio. A comparison of the partial admission results and the full admission results (ref. 5) is also made.

## SYMBOLS

$\Delta h$	turbine specific work, J/g
N	rotative speed, rpm
p	absolute pressure, N/cm <sup>2</sup>
$R_x$	blade reaction, $(w_5^2 - w_4^2)/2 \Delta h$
T	absolute temperature, K
U	blade velocity, m/sec
V	absolute gas velocity, m/sec
$\Delta V_u$	change in absolute tangential velocity, m/sec
W	relative gas velocity, m/sec
w	mass flow, kg/sec
$\alpha$	absolute gas flow angle measured from axial direction, deg
$\beta$	relative gas flow angle measured from axial direction, deg
$\Gamma$	torque, N-m
$\gamma$	ratio of specific heats
$\delta$	ratio of stator inlet total pressure to U. S. standard sea-level pressure, $p'_3/p^*$
$\epsilon$	function of $\gamma$ used in relating parameters to those using air inlet conditions at U. S. standard sea-level conditions, $(0.740/\gamma)[\gamma + 1]/2]^{(\gamma-1)}$
$\eta'$	efficiency based on total pressure ratio, $p'_3/p'_5$

$\theta$  circumferential position around scroll, deg  
 $\theta_{cr}$  squared ratio of critical velocity at stator inlet temperature to critical velocity at U.S. standard sea-level temperature,  $(V_{cr3}/V_{cr}^*)^2$   
 $\omega$  turbine speed, rad/sec

Subscripts:

cr critical corresponding to Mach number at unity

eq equivalent

1 station at scroll inlet (fig. 12)

3 station at stator inlet (fig. 12)

4 station at stator exit (fig. 12)

5 station at rotor exit (fig. 12)

6 station at diffuser exit (fig. 12)

Superscripts:

' absolute total state

\* U.S. standard sea-level conditions (temperature, 288.16 K; pressure, 10.13 N/cm<sup>2</sup>)

## TURBINE DESCRIPTION

A brief description of the full-scale turbine will be given first, followed by a description of the scale-model turbine. Engine design conditions for the full-scale turbine are presented in table I, along with the design equivalent conditions for the scaled turbine.

### Full-Scale Turbine

General description. - The full-scale turbine was designed to drive a lift-fan which has a nominal tip diameter of 152.4 centimeters. Figure 1 presents the basic layout of the fan and drive turbine. This figure is from reference 4. There are two inlets to the scroll which are located adjacent to each other. Each inlet is supplied by a separate gas generator and, in turn, each inlet supplies a different 180° segment of the scroll. The purpose of the dual inlets is for redundancy in case one of the gas generators fails.

Figure 1 shows axial and radial clearances in the turbine that are large compared to a conventional turbine design. These unusually large clearances are the result of large thermal growth of the scroll structure and to provide for considerable flexure of the fan. A three-chamber scroll was used to distribute the hot gas in the stator and to form a compact, structurally sound design. The lift-fan system was designed to be compact so that it could be enclosed within the envelope of the wing cross section.

A turbine exit diffuser was used to produce as low a static pressure as possible in the turbine rotor to prevent leakage of hot turbine gas into the fan.

Figure 2 shows the design mean-section velocity diagrams for the turbine. As discussed in reference 4, the turbine was a single-stage design with a supersonic stator and a subsonic, zero static pressure drop rotor. The turbine rotor had a hub-to-tip radius ratio of about 0.94. Both the stator and rotor blading were of constant section design.

Scroll. - The layout of the scroll flowpath for the reverse side of the turbine is shown in figure 3. As discussed in reference 4 the scroll is divided in half with each half supplied by separate inlets which are located adjacent to each other. This results in an air flow direction which is the same as the direction of rotor rotation in half of the scroll. This side of the scroll is called the forward side. In the other half of the scroll the airflow is in a direction opposite to that of rotation. This side of the scroll is called the reverse side. Figure 4 shows the relation of the forward and reverse sides to the direction of rotation. Each half is independent of the other half and serves  $180^{\circ}$  of the stator arc.

At each inlet the scroll is divided into three chambers. Only the large upper chamber continues around the full  $180^{\circ}$ . The design Mach number for the flow entering the scroll is approximately 0.3. The flow is then turned in the circumferential direction, divided into three chambers on each side, and accelerated to a Mach number of about 0.35. The flow then passes through a cascade of struts, which turns the flow radially into a vaneless annulus. This annulus then turns the flow axially into the stator assembly.

Stator. - Since the flow in one half of the scroll moves counter to the direction of rotation, three different vane profiles are used to meet the varying flow angles created by the scroll. Figure 5 shows the different vane types and how these vanes are located circumferentially with respect to the scroll. The vane profiles were designed for inlet flow angles of  $60^{\circ}$ ,  $0^{\circ}$ , and  $-60^{\circ}$ . However, the diverging portions of the passages were geometrically similar for all three types of vanes. The vanes were designed with a convergent-divergent flow passage which resulted in an exit-to-throat area ratio of 1.071. There was a total of 157 vanes.

Rotor. - Figure 6 shows the rotor blade profile. There was a total of 264 rotor blades. The rotor profile is constant from hub to tip. The rotor was designed to operate at impulse conditions to minimize the tip leakage losses. As mentioned previously, large axial and radial clearances are associated with fan flexure and shroud growth. The tip clearance is on the order of 1.3 centimeters, which is approximately 25 percent of

the rotor blade height. Thus, impulse blading with shrouded blade tips was chosen to minimize the tip leakage losses.

Diffuser. - The exit diffuser (fig. 1) consists of a diverging annular passage with eight struts. The struts serve as structural members to support the fan structure. The exit to inlet area ratio of the diffuser is approximately 1.5.

### Scale-Model Turbine

In order to test the LF460 turbine in an existing Lewis Research Center cold air component test facility, it was necessary to design and fabricate a 0.4 linear scale model of this turbine. Figure 7 is a photograph of the scaled turbine installed in the test cell. The photograph was taken from the exhaust end. Visible in this photograph is the inlet and exhaust piping and the scroll assembly.

Figure 8 is a closeup of the scroll and stator assembly in its mounting stand. The trailing edges of some of the stator vanes can be seen in this figure. The scroll chambers of the scaled turbine were rectangular rather than circular as in the full-size turbine. This change was made in order to simplify the fabrication.

The rotor is shown in figure 9. The rotor disk and blading were machined from a single forging, and a shroud ring was furnace-brazed to the blade tips. As discussed in the INTRODUCTION, the axial and radial tip clearances are scaled from the hot operating condition for the full-scale turbine.

### APPARATUS

The apparatus consisted of the turbine, a cradled gearbox, and a cradled dynamometer to absorb the power output of the turbine and to control turbine speed. In addition, there was inlet and exhaust piping with flow controls for setting inlet and exit pressures of the turbine. The arrangement of the apparatus is shown schematically in figure 10. High-pressure dry air was supplied from a central air system. The air passed through a 100-kilowatt heater, a calibrated orifice plate, and a remotely controlled turbine-inlet valve. Two valves, one in each of the two scroll inlets, were used to direct the air into one side of the scroll at a time. Leaving the turbine the air was exhausted through a system of piping and a remotely operated valve into a central low-pressure exhaust system. A 224-kilowatt dynamometer cradled on hydrostatic trunion bearings was used to absorb the turbine power, to control the turbine speed, and to measure the torque. The dynamometer was coupled to the turbine shafting through a gearbox cradled on hydrostatic bearings. The gearbox provided relative rotative speeds between dynamometer and turbine of 1.0 to 2.0. The stators of the gearbox and dynamometer were coupled together

so that the measured torque was the net torque developed by the turbine. Figure 11 shows the dynamometer and gearbox.

## INSTRUMENTATION

A torque arm attached to the dynamometer stator and a commercial strain-gage load cell were used to measure the net turbine torque. The load cell output was read on a digital voltmeter. The rotational speed was detected by a magnetic pickup and a shaft-mounted gear. The magnetic pickup output was converted to a direct-current voltage which was proportional to the frequency and fed into the digital voltmeter.

State conditions of the flow were determined by measurements taken at the scroll inlet, stator inlet, rotor exit, and diffuser exit. The instrumentation stations are shown in figure 12. The instrumentation at the scroll inlet (station 1) included four static pressure taps in each of the two inlets. A total-temperature rake containing three thermocouples was also located upstream of the two inlets. At the stator inlet (station 3) there were six static pressure taps equally spaced circumferentially along the hub wall. There were also six total pressure probes equally spaced circumferentially around the turbine. Each total pressure probe contained three elements to provide measurements at the mean radius and also near the hub and tip walls. In addition, there was a tube on each side of the mean-section total pressure sensing tube. These two side tubes had their sensing ends cut off to form a  $90^{\circ}$  wedge, and were connected to a differential pressure transducer to provide a means for manually alining the probe with the flow. A scale and pointer were attached to each probe to provide an indication of the mean-section flow angle.

At the rotor exit (station 5) there were 12 single-element Kiel total pressure probes approximately evenly spaced circumferentially. Radially these probes were spaced so that there were two each near the hub wall, the mean radius, and the tip wall on both the forward and reverse sides of the turbine. Use of Kiel type total pressure probes provided accurate total pressure readings over a range of absolute flow angle of about  $\pm 30^{\circ}$ .

At the diffuser exit (station 6) there were eight static pressure taps equally spaced circumferentially with four each at the inner and outer walls. Two self-alining probes, located  $180^{\circ}$  apart at the mean radius, were used for measurement of total pressure, total temperature, and flow angle.

For the partial admission tests the airflow was only through half of the turbine at a time. Therefore, only the instrumentation readings on the side of the turbine with the airflow were used for data reduction.

## PROCEDURE

The partial admission tests were conducted in two parts. In the first part the flow in the scroll was in the same direction as the direction of rotation. In the second part the airflow in the scroll was in a direction opposite to that of rotation. In both parts, data were obtained at nominal scroll inlet total conditions of 330 K and 9.60 newtons per square centimeter. Also in both parts, the tests were conducted over a range of speed from 40 to 140 percent of equivalent design speed, and over a range of scroll inlet total to diffuser exit static pressure ratio from 2.2 to 5.0.

Dynamometer-torque calibrations were obtained before and after each daily series of runs. Corrections were applied to the measured net turbine torque to include the effects of calculated disk windage and measured turbine bearing friction to obtain the turbine aerodynamic torque. At design conditions, these corrections amounted to about 2 percent of the measured turbine power.

The total efficiency  $\eta'$  was based on stator inlet total pressure and rotor exit total pressure. The stator inlet and rotor exit total pressures were an average of the respective measured values. At the scroll inlet, total pressure was calculated from mass flow, total temperature, static pressure, and flow angle. The rotor exit total temperature was calculated from the measured scroll inlet total temperature and the turbine specific work. When calculating the scroll inlet total pressure, the flow angle was assumed to be zero.

## RESULTS AND DISCUSSION

Partial admission performance results are presented for a 0.4 linear scale version of the LF460 lift fan turbine. These partial admission tests were conducted in two parts, with each part using a different side of the scroll to simulate loss of a gas generator. Each side had an arc of admission of  $180^\circ$ . In the first part, the forward side of the scroll was used in which the airflow was in the same direction as the direction of rotation. In the second part, the reverse side of the scroll was used in which the airflow was in a direction opposite to that of rotation. In both parts the performance tests were conducted at nominal scroll inlet total conditions of 330 K and 9.60 newtons per square centimeter. The range of speed covered in both parts was 40 to 140 percent of equivalent design speed, and the range of scroll inlet total to diffuser exit static pressure was 2.2 to 5.0.

Performance results are presented for both the forward and reverse sides. Results are presented as performance maps and curves relating equivalent values of mass flow and torque with pressure ratio. Table II compares several performance results from the partial admission and full admission investigations.

## FORWARD SIDE

### Mass Flow

Figure 13 shows the variation of equivalent mass flow  $\epsilon w \sqrt{\theta_{cr}} / \delta$  with total pressure ratio  $p'_3/p'_5$ . The figure indicates that the stator was choked over the range of speed and pressure ratio investigated. The equivalent choking mass flow was 1.747 kilograms per second, which represented about 52 percent of the mass flow obtained with full admission (table II). As discussed in reference 5, the full admission mass flow was approximately 10.1 percent greater than the design equivalent mass flow due to an oversized stator throat area.

### Torque

Figure 14 shows the variation of equivalent torque  $\epsilon \Gamma / \delta$  with total pressure ratio  $p'_3/p'_5$  for lines of constant speed. An equivalent torque of 189 newton-meters was obtained at equivalent design speed and pressure ratio. This value was approximately 48 percent of the full admission value (table II). Considering the percent changes in the mass flow and torque from their full admission values, it is apparent that the efficiency was approximately 8 percent less than the full admission value. The torque curves show a continuous increase with pressure ratio, indicating that limiting loading was not achieved.

### Performance Map and Calculated Turbine Velocity Diagrams

A performance map is shown in figure 15. This performance map is based on the total pressure ratio from the stator inlet to the rotor exit. The map shows equivalent specific work  $\Delta h / \theta_{cr}$  as a function of mass flow-speed parameter  $\epsilon w \omega / \delta$  for the various equivalent speeds investigated. Lines of constant pressure ratio  $p'_3/p'_5$  and efficiency  $\eta'$  are superimposed. An efficiency of about 0.750 was obtained at design equivalent speed and pressure ratio.

Figure 16 shows turbine velocity diagrams as calculated from experimental data at design equivalent speed and pressure ratio. These velocity diagrams were calculated based on mass-averaged conditions across the turbine. The velocity diagrams were constructed from the experimentally determined values of mass flow, torque, speed, stator inlet total pressure and total temperature, and rotor exit total pressure. In addition, two assumptions were used. The first assumption was specifying a value of 4.0 percent for the stator total pressure loss (table II). The second assumption was using a static

pressure on the upstream side of the rotor disk to represent the stator exit static pressure.

Values of rotor reaction  $R_x$  and rotor incidence angle were calculated using the velocity diagrams in figure 16. The rotor reaction was -0.065 compared to -0.031 for full admission. The rotor incidence angle was  $-0.1^\circ$  compared to  $1.9^\circ$  for full admission. These small deviations in reaction and incidence angle from their respective full admission values would be expected to have a negligible effect on the efficiency.

In addition, values of stator and rotor efficiency were calculated from the experimental velocity diagrams. The stator efficiency was 0.974. The stator efficiency is defined as the ratio of the actual stator exit kinetic energy to the ideal stator exit kinetic energy, which is a function of the stator inlet total to stator exit static pressure ratio. The rotor efficiency was 0.773. The rotor efficiency is defined as the ratio of the actual turbine work to the ideal turbine work, which is a function of the rotor inlet absolute total to rotor exit absolute total pressure ratio.

Figure 17(a) shows the circumferential variation of stator inlet total pressure. Total pressure measurements were made at the mean position and near the hub and tip walls at three different circumferential positions. At each circumferential position the hub, mean, and tip values were averaged. The overall circumferential average was 0.931 which represented a scroll total pressure loss of 6.9 percent. The variation in total pressure from positions A to C was similar for both full and partial admission operation. In both cases, the total pressure did not decrease uniformly from positions A to C as might have been expected. The reason for this unexpected deviation was not determined.

Figure 17(b) shows the circumferential variation of stator inlet mean flow angle. This flow angle was obtained at each position by manually alining the probe with the flow and using the pointer and scale that were attached to each probe to indicate the flow angle. The average flow angle was  $62^\circ$ , which was nearly identical to the average from positions A to C for full admission.

#### REVERSE SIDE

##### Mass Flow

Figure 18 shows the variation of equivalent mass flow  $\epsilon w \sqrt{\theta_{cr}/\delta}$  with total pressure ratio  $p'_3/p'_5$ . The figure indicates an equivalent choking mass flow of 1.632 kilograms per second, which represented about 49 percent of the mass flow obtained with full admission (table II). In addition, this choking mass flow was about 6.6 percent less than the value for the forward side. This difference in the equivalent mass flow rates between

the forward and reverse sides was attributed to a larger total stator vane throat area for the forward side and a larger stator total pressure loss for the reverse side.

### Torque

Figure 19 shows the variation of equivalent torque  $\epsilon \Gamma / \delta$  with total pressure ratio  $p'_3/p'_5$  for lines of constant speed. An equivalent torque of 172 newton-meters was obtained at equivalent design speed and pressure ratio. This value was approximately 44 percent of the full admission value (table II), and was 9 percent less than the value for the forward side. Considering the percent changes in the mass flow and torque from their full admission values, it is apparent that the efficiency was about 10 percent less than the full admission value and 2 percentage points less than the efficiency for the forward side.

### Performance Map and Calculated Turbine Velocity Diagrams

Figure 20 shows a performance map based on the total pressure ratio from the stator inlet to the rotor exit. This map is similar to figure 15 for the forward side. At design equivalent speed and pressure ratio an efficiency of about 0.730 was obtained. As mentioned previously, this was 2 percentage points less than the efficiency for the forward side. Since the arc of admission for both the forward and reverse sides was  $180^\circ$ , the partial admission losses should have been the same. Therefore, the difference in efficiency was attributed to larger stator losses on the reverse side. Referring to figure 5, it can be seen that the type III stator vanes have almost  $126^\circ$  of total flow turning compared to only about  $6^\circ$  of flow turning for the type I stator vanes. Therefore, the type III vanes would be more susceptible to incidence effects at the leading edge. This could lead to flow separation and higher stator total pressure losses.

Turbine velocity diagrams as calculated from experimental data at design speed and pressure ratio were also computed for the reverse side. These diagrams are shown in figure 21. The velocity diagrams were calculated using the same method as for the forward side. For the reverse side, however, a stator total pressure loss of 5.6 percent was assumed. Again, values of rotor reaction  $R_x$  and rotor incidence angle were computed. The rotor reaction was -0.131 and the rotor incidence angle was  $2.2^\circ$ . The corresponding differences with the forward side values were small. Also, values of stator and rotor efficiency were calculated. The stator efficiency was 0.964 and the rotor efficiency was 0.759. Both efficiencies decreased by about 0.010 from their corresponding forward side values. This decrease was attributed primarily to the effects of the higher stator total pressure loss.

Figure 22(a) shows the circumferential variation of stator inlet total pressure. The overall circumferential average was 0.946, which represented a scroll total pressure loss of 5.4 percent. The variation in total pressure from positions D to F was similar for both full and partial admission operation.

Figure 22(b) shows the circumferential variation of stator inlet mean flow angle. The average flow angle was  $54.3^{\circ}$  which was nearly identical to the average from positions D to F for full admission. However, more importantly, from positions E to F there was  $10^{\circ}$  to  $15^{\circ}$  of negative incidence (using the design inlet mean flow angle to represent the blade angle). This probably resulted in flow separation, thereby causing larger stator losses and a lower efficiency on the reverse side.

### Comparison of Full and Partial Admission Results

For the purpose of comparing the efficiencies between full and partial admission, an average partial admission efficiency of 0.740 was calculated by averaging the efficiencies for the forward and reverse sides. Calculating an average partial admission efficiency appeared reasonable since the full admission efficiency of 0.815 (table II) represents an average of the forward and reverse sides without any partial admission losses. These partial admission losses accounted for the approximate 9 percent decrease in efficiency between full and partial admission. As discussed in reference 6, the partial admission losses usually considered are the pumping loss in the inactive blade channels and the filling-and-emptying loss in the blade passages as they pass through the admission arc. This latter loss is also referred to as expansion, scavenging, or sector loss.

Although analytical expressions exist for these losses, the empirical loss coefficients needed in these expressions are questionable. Therefore, reasonable agreement between these loss expressions and experimental data is not always obtained.

To provide a comparison with the partial admission results from the LF460 turbine, the experimental results from the investigation of reference 7 were used. The turbine used in this investigation was a single-stage, axial-flow turbine with a mean diameter of about 9.5 centimeters. The tests covered admission values of 100, 51, 31, and 12 percent. At design blade-jet speed ratio and an admission value of 51 percent, a decrease in turbine static efficiency of about 6 percent was obtained. This report based its comparisons only on turbine static efficiency. For this reference turbine a decrease in static efficiency of 9 percent was associated with an admission value of approximately 20 percent.

## SUMMARY OF RESULTS

Partial admission performance was obtained for a 0.4 linear scale of the LF460 lift fan turbine over a range of speed and pressure ratio. These cold-air tests were conducted in two parts, with each part using a different side of the turbine scroll to simulate loss of a gas generator. Each side had an arc of admission of 180°. In the first part the forward side of the scroll in which the airflow was in the same direction as the direction of rotation was used. In the second part the reverse side of the scroll in which the airflow was in a direction opposite to that of rotation was used. The results of this investigation may be summarized as follows:

1. An efficiency of 0.750 was obtained on the forward side of the turbine at design equivalent speed and pressure ratio. This efficiency is based on the total pressure ratio from the stator inlet to the rotor exit.
2. An efficiency of 0.730 was obtained on the reverse side of the turbine at design equivalent speed and pressure ratio. The difference in efficiency between the forward and reverse sides was attributed to higher stator losses on the reverse side of the turbine.
3. An average partial admission efficiency of 0.740 was obtained by averaging the efficiencies of the forward and reverse sides. This average efficiency was 9 percent less than the efficiency obtained with full admission. The decrease in efficiency was attributed to the pumping and sector losses associated with partial admission operation.

Lewis Research Center,  
National Aeronautics and Space Administration,  
and  
U.S. Army Air Mobility R&D Laboratory,  
Cleveland, Ohio, October 29, 1976,  
505-05.

## REFERENCES

1. Novak, L. R.: The Lift/Cruise Fan Multimission V/STOL Aircraft. AIAA Paper 75-277, Feb. 1975.
2. Dugan, James F., Jr.; et al.: Preliminary Study of an Air Generator - Remote Lift Fan System for VTOL Transports. NASA TM X-67916, 1971.
3. Gertsma, L. W.; and Zigan, S.: Propulsion System for Research VTOL Transports. ASME Paper 73-GT-24, Apr. 1973.
4. LF460 Detail Design. (General Electric Co.; NAS2-6056), NASA CR-120787, 1971.

5. Haas, Jeffrey E.; et al.: Cold-Air Performance of a Tip Turbine Designed to Drive a Lift Fan. I - Baseline Performance. NASA TM X-3452, 1976.
6. Glassman, Arthur J., ed.: Turbine Design and Application. Vol. II, NASA SP-290, 1973, pp. 138-143.
7. Klassen, Hugh A.: Cold-Air Investigation of Effects of Partial Admission on Performance of 3.75-Inch-Mean-Diameter Single-Stage Axial-Flow Turbine. NASA TN D-4700, 1968.

TABLE I. - TURBINE DESIGN CONDITIONS

Parameter	Engine (full scale)	Equivalent (0.4 scale)
Stator inlet temperature, $T_3'$ , K	1 144	288.2
Stator inlet pressure, $p_3'$ , N/cm <sup>2</sup>	37.7	10.13
Mass flow rate, w, kg/sec	34.6	3.03
Rotative speed, N, rpm	4 300	5 395
Specific work, $\Delta h$ , J/g	268.4	67.6
Torque, $\Gamma$ , N-m	20 623	363
Power, kW	9 290	205
Pressure ratio, $p_3'/p_5'$	3.05	3.16
Pressure ratio, $p_1'/p_6$	3.92	4.10
Efficiency, $\eta'$	0.832	0.832
Work factor, $\Delta V_u/U$	1.982	1.982

TABLE II. - COMPARISON OF TURBINE PERFORMANCE FOR  
FULL AND PARTIAL ADMISSION OPERATION

Parameter	Partial admission		Full admission (ref. 5)
	Forward side	Reverse side	
Equivalent mass flow, $\epsilon w \sqrt{\theta} / \delta$ , kg/sec	1.747	1.632	3.336
Equivalent torque, $\epsilon \Gamma / \delta$ , N-m	189	172	392
Scroll inlet total pressure, $p_1'$ , N/cm <sup>2</sup>	9.56	9.53	9.09
Scroll total pressure loss, $\frac{p_1' - p_3'}{p_1'}$ , percent (measured)	6.9	5.4	6.4
Stator total pressure loss, $\frac{p_3' - p_4'}{p_3'}$ , percent (assumed)	4.0	5.6	4.8
Efficiency, $\eta'$	0.750	0.730	0.815

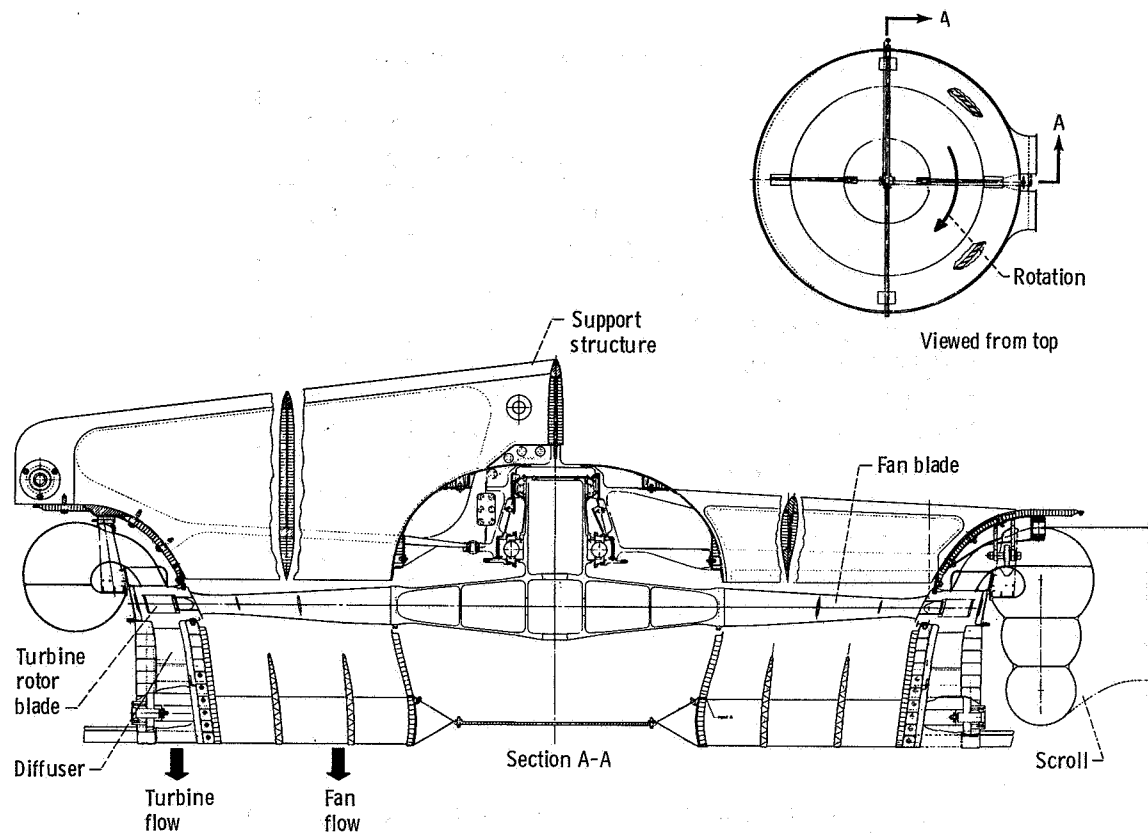


Figure 1. - Lift-fan assembly.

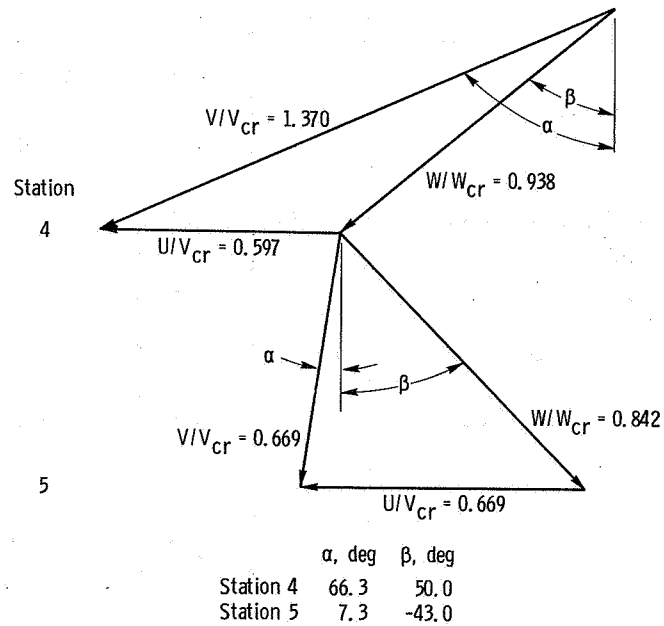


Figure 2. - Design velocity diagrams for LF460 turbine at mean section.

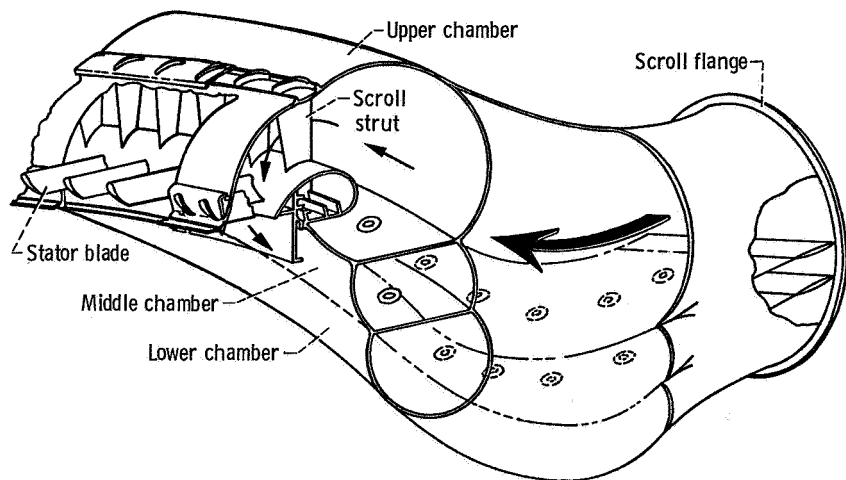


Figure 3. - Scroll flowpath for reverse side of turbine.

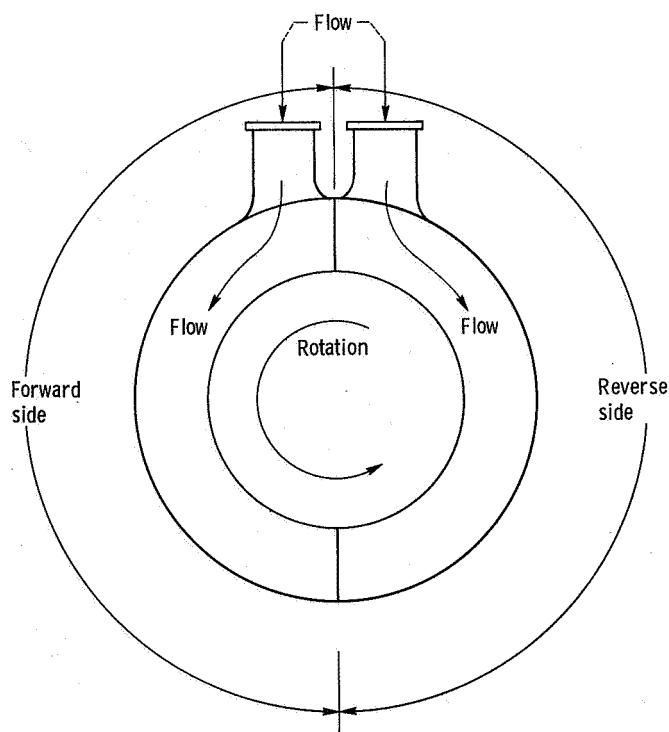


Figure 4. - Forward and reverse sides of turbine (viewed from exhaust end).

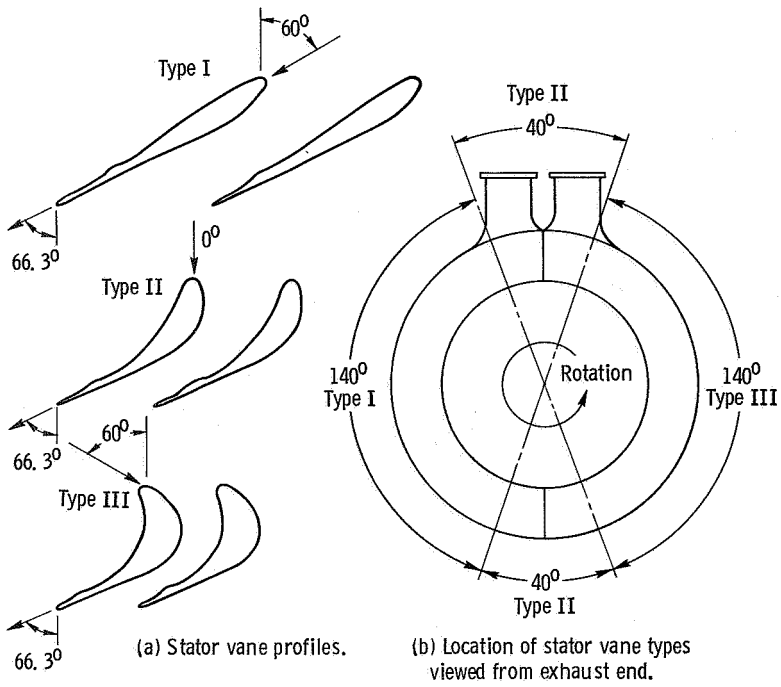


Figure 5. - Stator vane profiles and locations.

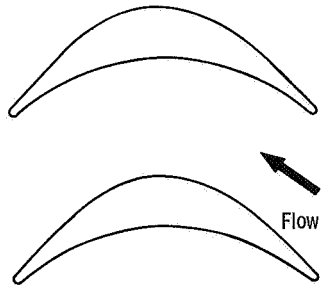


Figure 6. - Rotor blade profile.

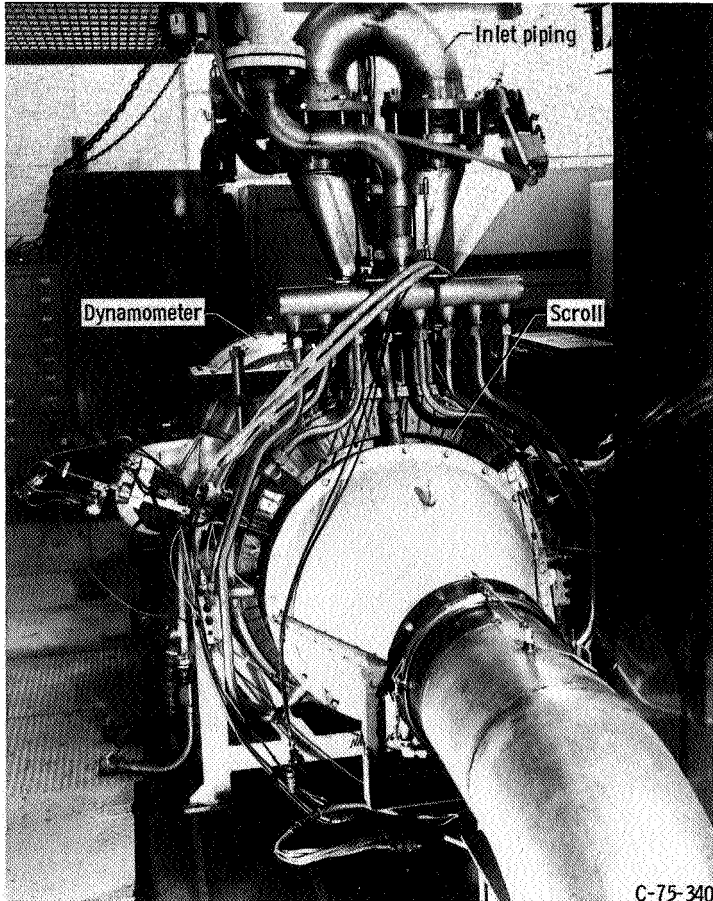


Figure 7. - Turbine test installation.

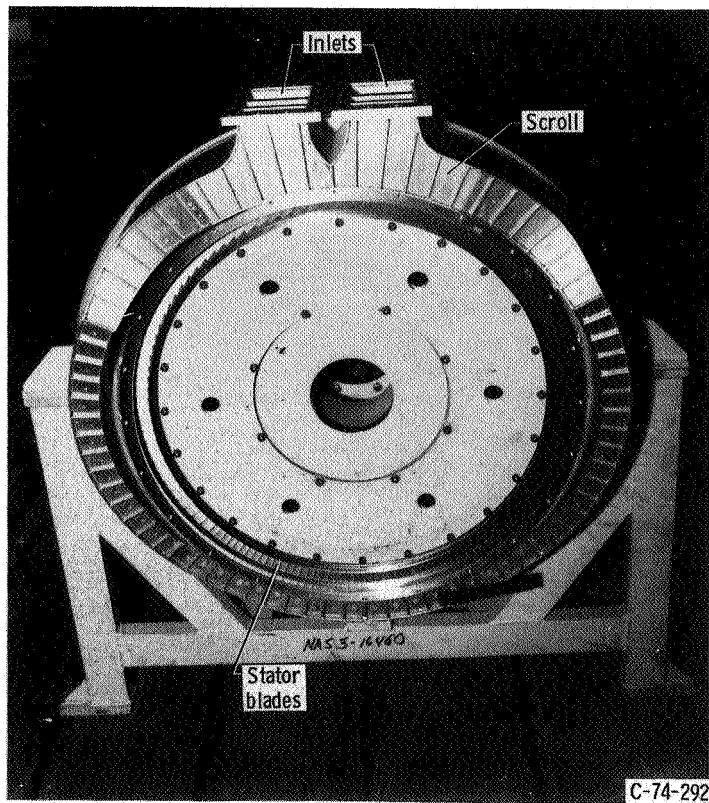


Figure 8. - Test scroll and stator.

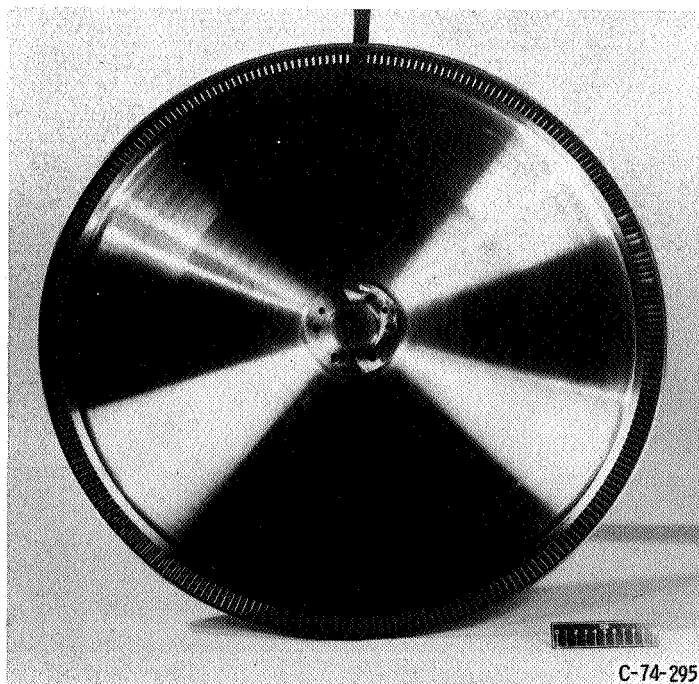


Figure 9. - Test rotor.

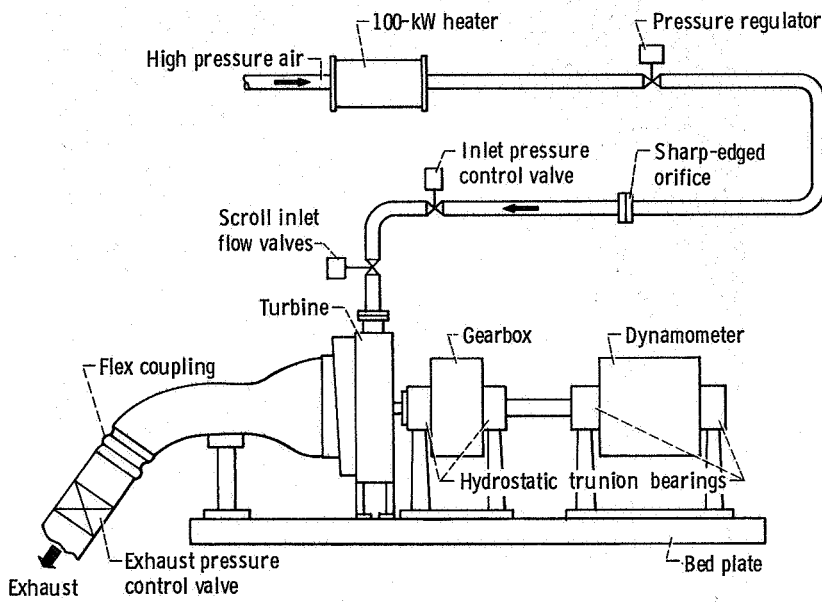


Figure 10. - Test installation diagram.

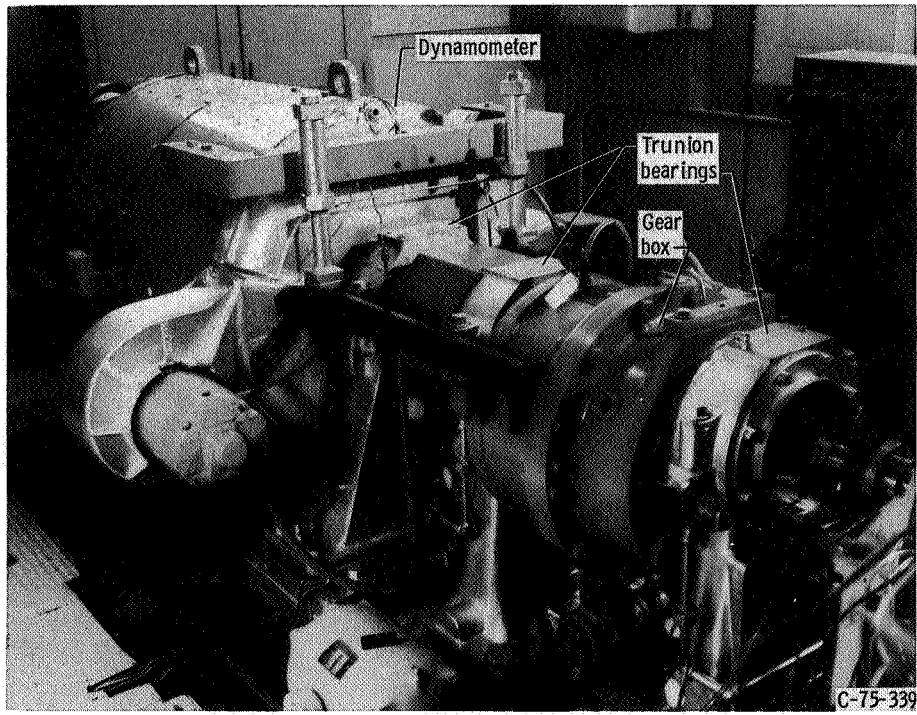


Figure 11. - Dynamometer and gearbox.

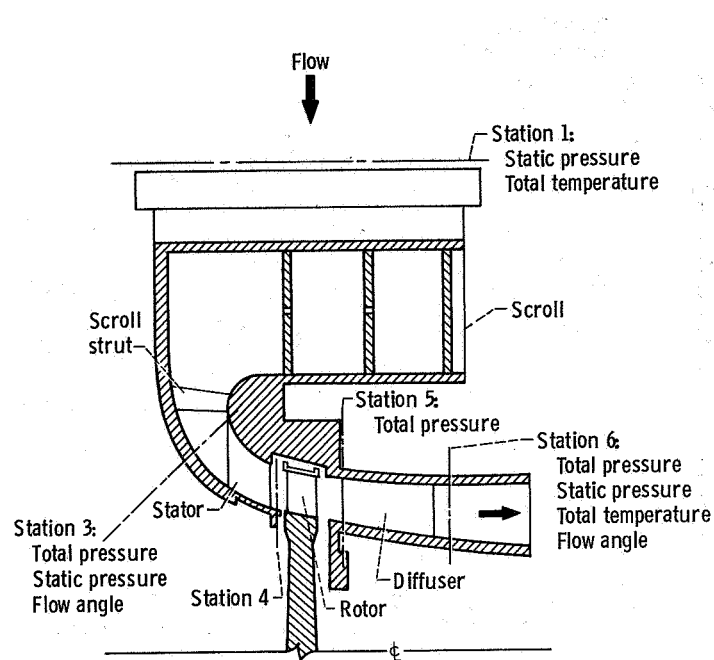


Figure 12. - Turbine showing instrumentation stations.

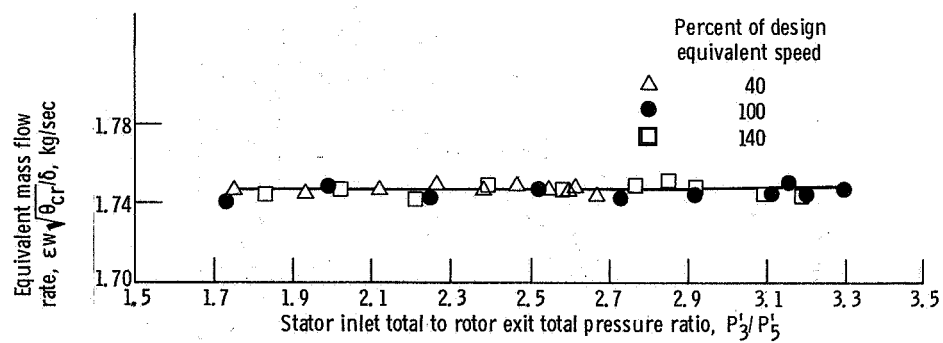


Figure 13. - Variation of mass flow with pressure ratio for forward side of turbine.

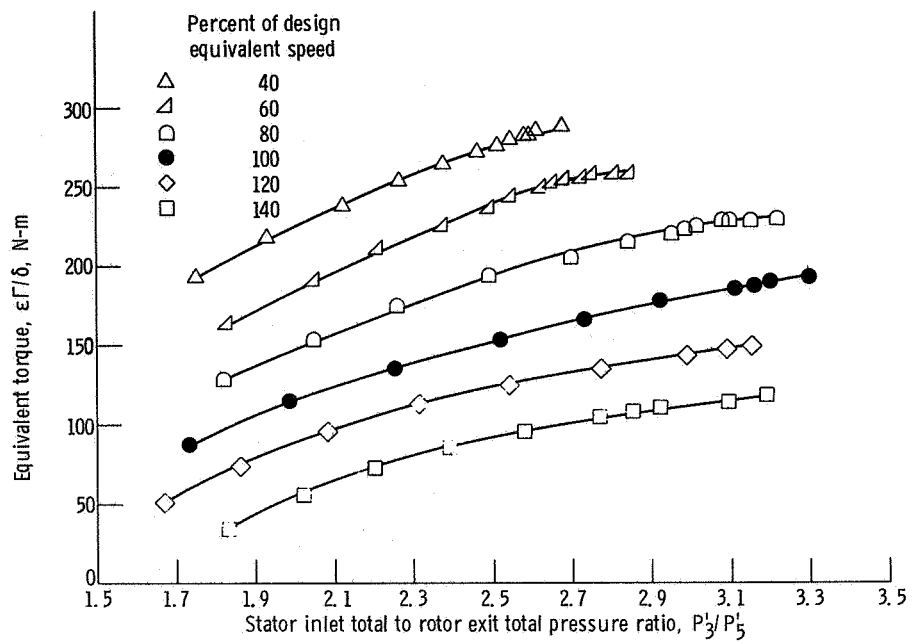


Figure 14. - Variation of torque with pressure ratio for forward side of turbine.

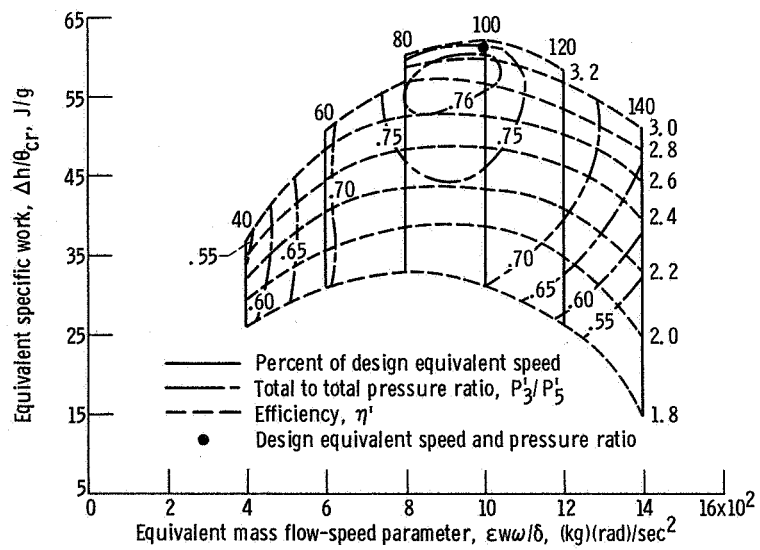


Figure 15. - Performance map based on flow conditions at stator inlet and rotor exit for forward side of turbine.

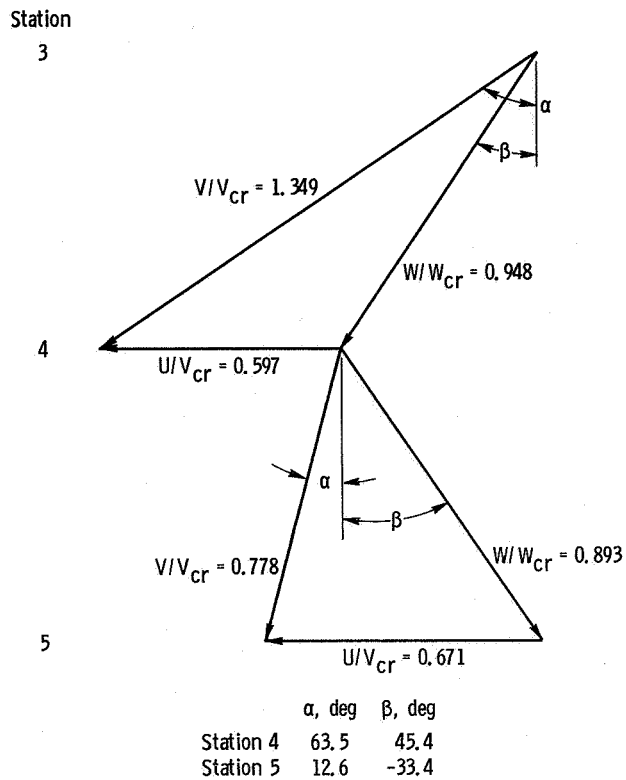


Figure 16. - Velocity diagrams as calculated from experimental results at design equivalent speed and pressure ratio for forward side of turbine.

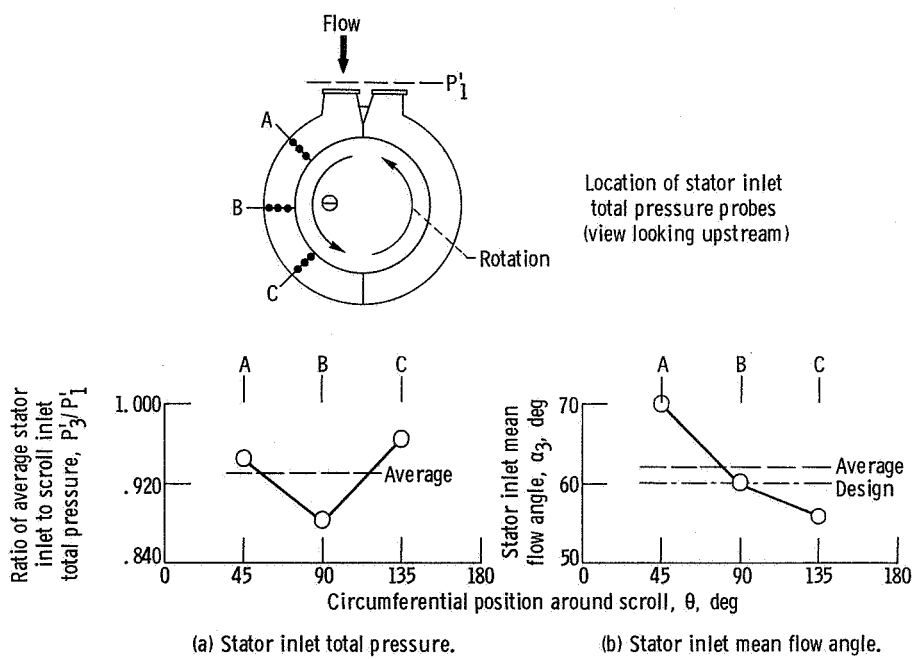


Figure 17. - Variation of stator inlet mean flow angle and total pressure with circumferential position for forward side of turbine.

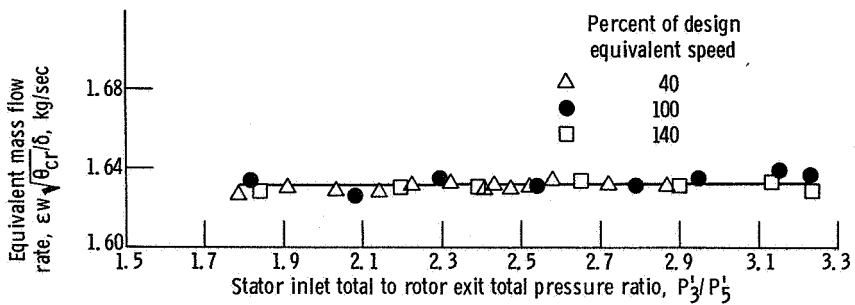


Figure 18. - Variation of mass flow with pressure ratio for reverse side of turbine.

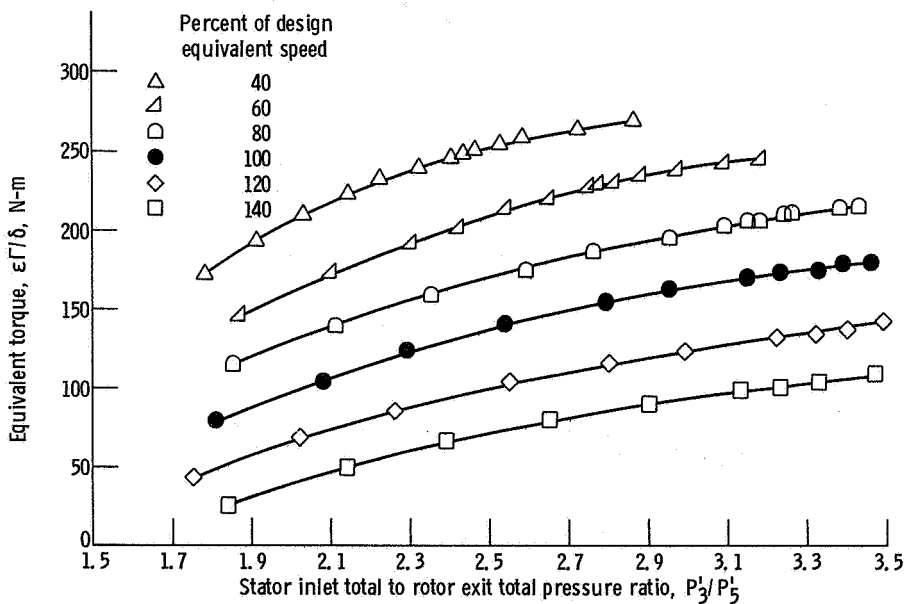


Figure 19. - Variation of torque with pressure ratio for reverse side of turbine.

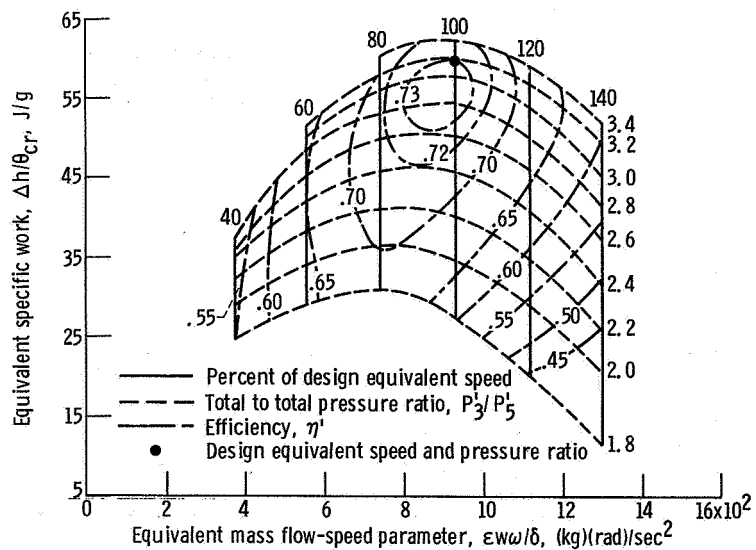


Figure 20. - Performance map based on flow conditions at stator inlet and rotor exit for reverse side of turbine.

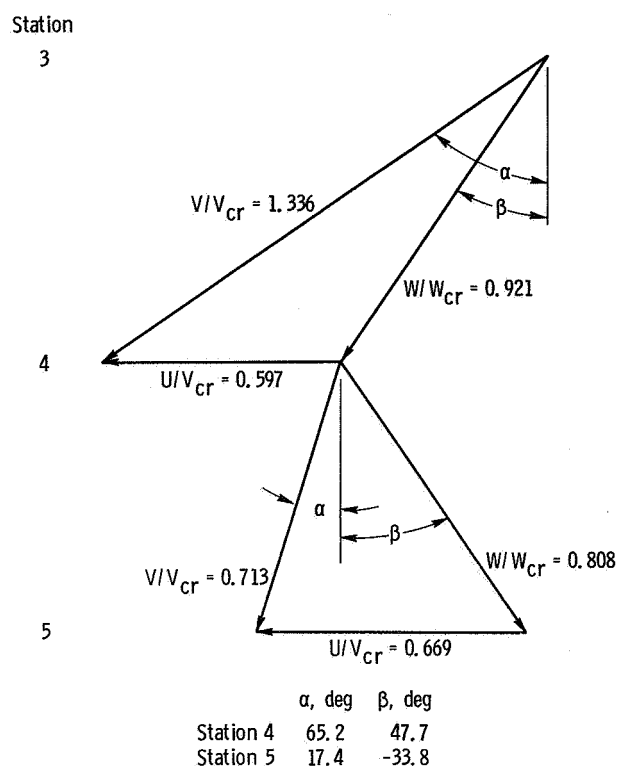


Figure 21. - Velocity diagrams as calculated from experimental data at design equivalent speed and pressure ratio for reverse side of turbine.

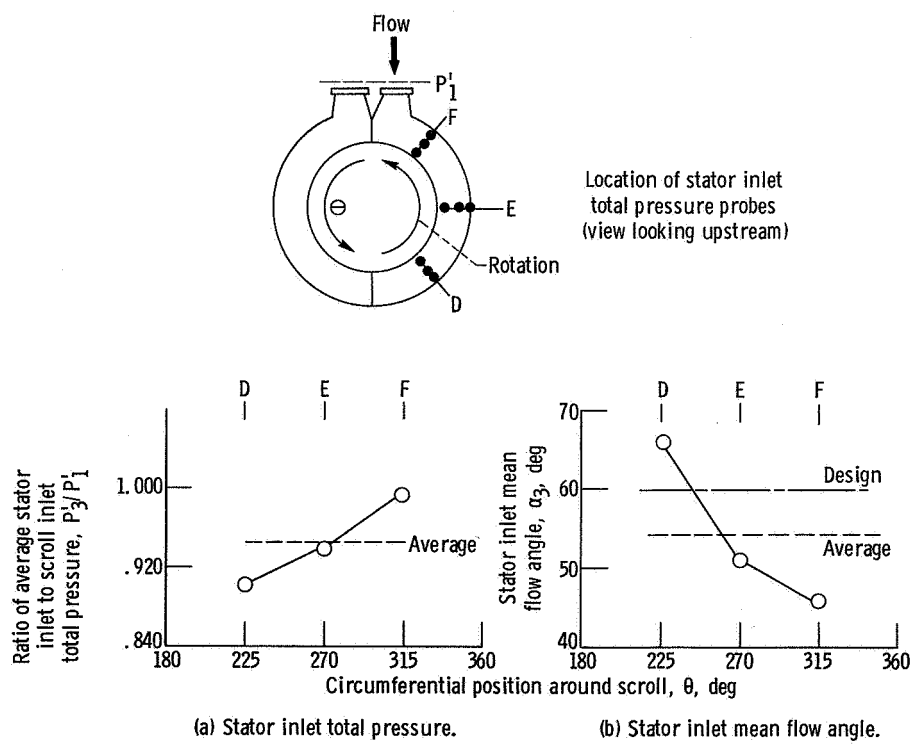


Figure 22. - Variation of stator inlet mean flow angle and total pressure with circumferential position for reverse side of turbine.